镀锌薄板TIG拼焊的焊缝组织及成形性能

彭本栋[1]， 张 建[1]， 李云涛[1]， 杨立军[2]， 刘广达[1]
（1. 天津理工大学 材料科学与工程学院，天津 300191；
2. 天津大学 材料科学与工程学院，天津 300072）


彭本栋

摘 要：采用钨极惰性气体焊对镀锌薄板SGCC实施等厚拼焊，测试分析了拼焊板焊接接头的金相组织、显微硬度，并对拼焊板和母材试样进行杯突试验．结果表明，在拼焊过程中，母材的散热情况不同会造成焊缝金相组织在靠近母材的局部区域有很大差异．焊缝熔合区组织为粗的片状与块状先共析铁素体沿柱状晶界分布，晶内为魏氏体组织和片状珠光体，热影响区为块状的珠光体和铁素体，导致了焊缝及其热影响区的硬度均高于母材，对拼焊板的整体成形性能产生负面影响；同时，焊缝杯突值较母材有一定程度的降低，揭示其焊缝深冲性能低于母材．

关键词：镀锌薄板；钨极惰性气体焊；微观组织；杯突试验
中图分类号：TG456.7 文献标识码：A 文章编号：0253－360X(2009)12－0082－03

0 序 言

拼焊板是指在冲压成形前将两块或两块以上不同厚度、不同材质或不同表面涂层的板材采用焊接方法拼在一起而形成的冲压用平板坯料[1,2]．拼焊板技术具有节省材料、减少零件数量、降低车重，从而降低油耗、提高整体性能及保护环境等优势，在汽车行业中应用前景广阔[3－5]．

随着汽车工业的发展，对车身的防腐要求也提高了，而镀锌板本身具有良好的防腐蚀特性，因此在汽车车身上得到广泛应用[6]．将拼焊板技术应用到镀锌板冲压成形中，结合两者的优势，是近年来汽车设计和制造的热点之一．鉴于此文中采用钨极惰性气体(tungsten inert gas，TIG)焊接方法对等厚的镀锌薄板进行拼焊，然后进行拼焊板微观组织、硬度、杯突试验．

1 试验方法

试验材料为日本牌号的SGCC镀锌板，板厚为0.7 mm，其化学成分如表1所示．

电焊机为林肯275逆变式焊机，接头为平板对接，无填充焊丝．主要焊接工艺参数如表2所示．

表1 镀锌板的化学成分(质量分数，%)
Table 1 Chemical compositions of galvanized sheet

C	Si	Mn	P	S	Al
0.06	0.02	0.22	0.02	0.02	余量

表2 焊接工艺参数
Table 2 Welding parameters of TIG

焊接速度 v/(m·min^{-1})	焊接电流 I/A	电流种类	电弧电压 U/V	电弧长度 L/mm
1.88	180	直流正接	12	2～3

钨极直径 D/mm	喷嘴直径 d/mm	保护气体	保护气体流量 q/(L·min^{-1})
4	8	Ar	12

在SGCC拼焊板上选取具有代表性的焊缝横截面进行金相组织分析；采用HMV－2T型显微硬度计对焊缝接头各区域进行硬度测量；采用数显半自动杯突试验机对焊缝部位进行杯突试验(GB/T4156－1984)，检验焊缝区深冲性能，分析SGCC拼焊板杯突试验中的成形特点及焊缝对成形性能的影响．TIG焊实施的拼焊板如图1所示．

2 试验结果与分析

2.1 焊接接头微观组织测试及分析

SGCC拼焊板焊接接头显微组织测试结果如图2所示．

收稿日期：2008－07－22
基金项目：天津市科技支撑计划资助项目(07ZCKFGX02400)；天津市应用基础研究计划资助项目(07JCYBJ04400)

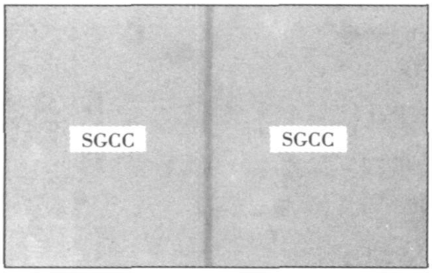

图 1　拼焊板

Fig　1　Tailor welded blank

图 2a 为镀锌板 TIG 焊缝金相组织形貌,焊缝中分布着粗大的片状、块状先共析铁素体以及粗大的针状铁素体组织,少量的柱状魏氏体组织.

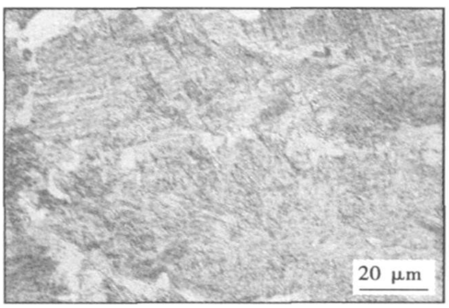

(a) 焊缝组织形貌

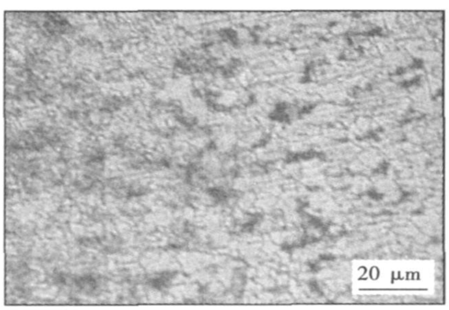

(b) 热影响区组织形貌

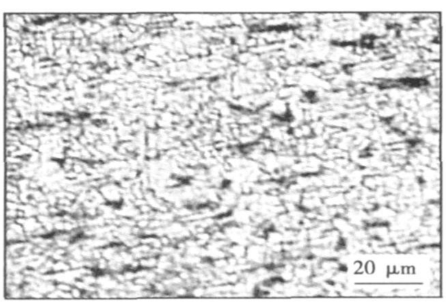

(c) 母材SGCC组织形貌

图 2　SGCC 拼焊板焊接接头组织形貌

Fig　2　Microstructure of SGCC and welding joint

图 2b 为焊接接头热影响区金相组织形貌,其中图左侧为完全重结晶区,该区域为细小而均匀的铁素体和珠光体;中间区域为不完全重结晶区,该区域为珠光体和铁素体,并且晶粒大小不一,组织不均匀. 图右侧为母材侧.

图 2c 为镀锌板焊接母材组织形貌,镀锌板的母材组织为块状铁素体和少量的珠光体.

2.2　焊接接头显微硬度分析

SGCC 拼焊板焊接接头沿垂直焊缝方向的硬度分布如图 3 所示. 可以看出,SGCC 焊接接头的硬度以焊缝中心线为轴呈近似对称分布,焊缝区宽度约为 3 mm,焊缝处的硬度要高于母材,焊缝中心处硬度较低为 227 HV,但仍高于母材. 从焊缝中心处到母材 SGCC 侧焊缝硬度先是不断的升高,在距离焊缝中心约 0.5 mm 处,焊缝的硬度达到最高值 324 HV,然后焊缝的硬度逐渐下降,最终达到原始母材 SGCC 的硬度. 焊缝及其热影响区的硬度均高于母材,这对拼焊板的整体成形性能会产生负面影响.

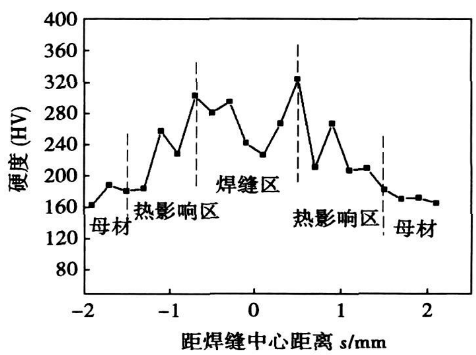

图 3　TIG 焊焊接接头硬度分布

Fig.　3　Hardness distribution of welded joint

2.3　焊接接头及母材杯突试验

杯突试验试样尺寸如图 4 所示[7,8],分别对焊缝区和母材试样进行杯突试验. 母材 SGCC 的杯突值为 9.56 mm,拼焊板的杯突值为 6.92 mm.

杯突试验结果如图 5 所示,由试验结果可知,拼焊板的杯突值要低于母材的杯突值,说明焊缝深冲性能低于母材. 这是由于焊接热循环的作用,焊缝晶粒有不同程度的长大,所以焊缝区晶粒比母材粗大,造成焊缝部位塑性和韧性下降.

杯突试验过程中由于拼焊板为相同材料的等厚拼焊板,焊缝位于拼焊板的中心线,焊缝两侧板的变形一致,裂纹扩展速度相等,裂纹在两侧板中的长度相同. 在相同的压力下两侧板材的应变相同,焊缝不发生偏移. 且焊缝的加强筋作用明显,焊缝两边材料变形的相互影响较小,裂纹从焊缝处开裂,且焊

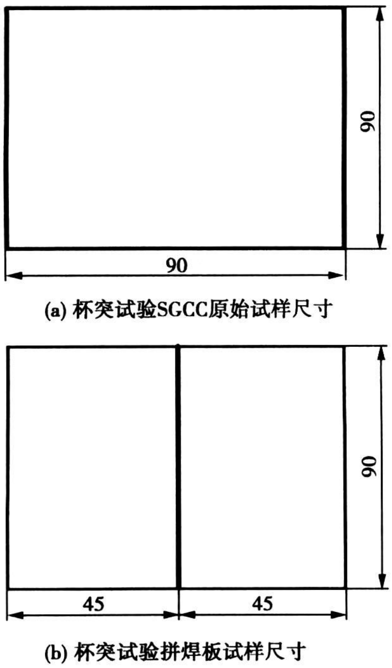

图 4 杯突试验试样尺寸(mm)

Fig. 4 Profile and dimensions of cupping test specimens

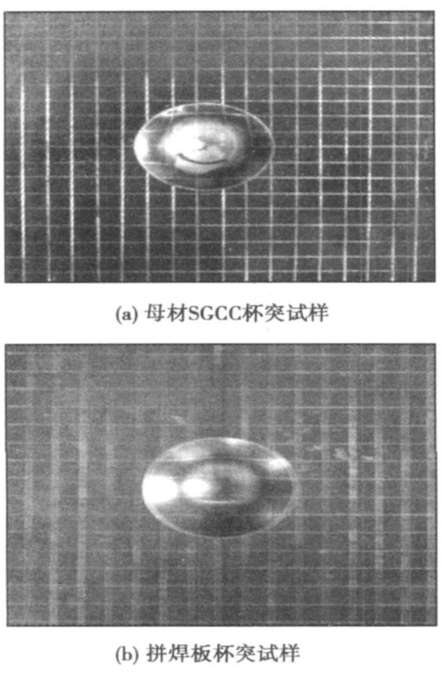

图 5 拼焊板杯突试验结果

Fig. 5 Results of cupping test

缝两侧的裂纹长度相等, 裂纹呈环形.

在冲压成形过程中, 由于焊缝加强筋的作用会阻碍强烈变形区材料的塑性流动, 降低拼焊试样的成形能力, 因此成形过程中应避免使焊缝处于强烈变形区.

3 结 论

(1) 焊缝中存在沿柱状晶界分布的粗大的片状、块状先共析铁素体, 晶内为魏氏体组织、铁素体和片状珠光体. 热影响区为块状珠光体和铁素体.

(2) 焊缝处的硬度值要高于母材处的硬度, 焊缝中心处的硬度为 227 HV. 从焊缝中心处到母材侧焊缝硬度先是不断的升高, 在距离焊缝中心约 0.5 mm 处, 焊缝的硬度达到最高值 324 HV.

(3) 拼焊板的杯突值要低于母材的杯突值, 说明拼焊板的胀形性低于母材; 焊缝没有发生偏移, 基本上没有发生变形, 焊缝仍保持直线形; 焊缝的加强筋作用明显, 将阻碍强烈变形区材料的塑性流动, 成形过程中应避免让焊缝流入强烈变形区.

参考文献:

[1] 崔怀洋, 左铁钏. 激光焊接的裁焊板及其在汽车中的应用[J]. 焊接技术, 2004, 33(1): 23−26.
Cui Huaiyang, Zuo Tiechuan. Tailored laser-welded blanks and its application in automobile manufacturing[J]. Welding Technology, 2004, 33(1): 23−26.

[2] 瞿 丰, 邓正才, 姚 舜, 等. 汽车拼板的激光焊接的研究[J]. 焊接技术, 2003, 23(5): 27−29.
Qu Feng, Deng Zhengcai, Yao Shun, *et al*. Research on laser welding of tailored-blank[J]. Welding Technology, 2003, 23(5): 27−29.

[3] 林建平, 孙东继, 胡巧声, 等. 汽车用拼焊板国内外研究进展[J]. 汽车技术, 2007(8): 1−5.
Lin Jianping, Sun Dongji, Hu Qiaosheng, *et al*. Development of research in tailor welded blanks used in auto industry[J]. Automobile Technology, 2007(8): 1−5.

[4] 姜银方, 杨继昌, 陈 炜. 拼焊板冲压成形研究的现状和发展趋势[J]. 汽车工程, 2003, 25(4): 410−414.
Jiang Yinfang, Yang Jichang, Chen Wei. The status quo and trends of tailor welded blanks [J]. Automotive Engineering, 2003, 25(4): 410−414.

[5] 李淑慧, 林忠钦, 倪 军, 等. 拼焊板在车身覆盖件冲压成形中的研究进展[J]. 机械工程学报, 2002, 38(2): 1−5.
Li Shuhui, Lin Zhongqin, Ni Jun, *et al*. Current development and trends of the tailored blank application in autobody stamping[J]. Chinese Journal of Mechanical Engineering, 2002, 38(2): 1−5.

[6] Tusek J, Kampus Z, Suban M. Welding of tailored blanks of differernt materials[J]. Journal of Materials Processing Technology, 2001, 119(1−3): 180−184.

[7] 童正国. 拼焊板胀形成形不均匀性研究及数值仿真[D]. 上海: 同济大学, 2006.

[8] Meinders T, A van den Berg, Huetink J. Deep drawing simulations of tailored blanks and experimental verification[J]. Journal of Metarials Processing Technology, 2000, 103(1): 65−73.

作者简介: 彭本栋, 男, 1981 年出生, 硕士研究生. 主要从事汽车轻量化板材成形性能方面的研究工作. 发表论文 1 篇.
Email: cherypbd@163.com

by using blowhole resistance as function and computer software, and then the trend diagrams of effects of every ingredient and the mathematical model between blowhole resistance of stainless steel electrode and 11 coating components were given. The effect of feldspar and muscovite on the mark of blowhole resistance is positive by trend diagrams. There are interactions between most coating components and blowhole resistance by mathematical model. The searching and forecasting can be done by using mathematical model and computer program.

Key words: stainless steel electrode; new slag system; blowhole; uniform design

Numerical simulation on thermal fatigue behavior of CuCGA soldered joints

XIAO Zhengxiang[1], XUE Songbai[1], JIN Chunyu[2], ZHANG Liang[1], GAO Lili[1] (1. College of Materials Science and Technology, Nanjing University of Aeronautics and Astronautics, Nanjing 210016, China; 2. College of Mathematical Sciences, Heilongjiang University, Haerbin 150080, China). p 77—81

Abstract: The constitutive equation of Sn3.9Ag0.6Cu and 63Sn37Pb were established based on creep law, and the stress-strain distribution of soldered joints in copper column grid array (CuCGA) devices was analyzed under the loadings of different temperature cycles. Results indicate that no matter how the change of temperature cycle range, the maximum creep strain is located in the soldered joint where the location from the device center is foremost, in which the stress concentration is found and cracks appear, therefore, the corner soldered joint is the most fragile area in the whole device. Creep strain of Sn3.9Ag0.6Cu soldered joints is smaller than that of 63Sn37Pb soldered joints. Lower stress and creep strain are exhibited for both Sn3.9Ag0.6Cu and 63Sn37Pb when the temperature cycles range is shortened. Sn3.9Ag0.6Cu soldered joints show higher thermal fatigue life than 63Sn37Pb soldered joints under the same temperature cycle.

Key words: copper column grid array; reliability; creep law; fatigue life

Formability and microstructure characteristics of galvanized plate by TIG welding

PENG Bendong[1], ZHANG Jian[1], LI Yuntao[1], YANG Lijun[2], LIU Guangda[1] (1. School of Materials Science and Engineering, Tianjin University of Technology, Tianjin 300191, China; 2. School of Materials Science and Engineering, Tianjin University, Tianjin 300191, China). p 82—84

Abstract: The microstructure and micro-hardness of welded joint of SGCC by tungsten inert-gas (TIG) welding are studied, and the cupping test of Tailor-welded blank and base metal are studied. The results show that in the welding process, the microstructure of weld will have great diversity at local region closing parent metal because of the different cooling condition of the parent metal. The microstructure of welding fusion zone is massive sheet proeutectoid ferrite distribution along the columnar grain boundaries, intragranular organizations are Widmanstatten and sheet pearlite structure, and the microstructure in HAZ is massive pearlite and ferrite, which make the micro-hardness value of welding seam and HAZ higher than that of base metal and lead negative influence to the formability of Tailor-welded blank. The cupping value of weld seam reduces to some extent compared with that of base metal, which indicates that the formability of weld seam is not good as that of base metal.

Key words: galvanized sheet; TIG welding; microstructures; cupping test

Welding experiment on 1Cr18Ni9Ti and 1Cr13 stainless steels

ZHAO Yongtao[1], DONG Junhui[2], ZHAO Liping[1], MA Yonglin[1], PEI Xiaobing[1] (1. Material and Metallurgy Engineering School, UST Inner Mongolia, Baotou 014010, China; 2. Materials Science and Engineering, Inner Mongolia University of Technology, Huhhot 010051, China). p 85—88

Abstract: The stainless steels of 1Cr18Ni9Ti and 1Cr13 were welded through deterministic craft by tungsten inert-gas (TIG) welding. The microstructure and fracture pattern of weld joints of 1Cr13 martensite and 1Cr18Ni9Ti austenite stainless steels were observed and analyzed by means of LOM and SEM, the mechanical properties of the weld joints were measured with micro-hardness tester and electronic universal stretcher, and the polarization curves and AC impedance spectroscopy of weld joints were tested by seawater immersion test of simulation solution. The results show that adopting manual TIG welding through electrode negative to direct current soldering machine to weld 1Cr18Ni9Ti austenite stainless steel and 1Cr13 martensite stainless steel is feasible; under suitable process (welding current is 80 A, welding speed is 110 mm/min), weld joints can obtain good appearance and uniform structure; mechanical properties and galvano-chemistry properties can meet use requirements.

Key words: 1Cr13; 1Cr18Ni9Ti; welding joint; microstructure and properties

Microstructures and properties of Ti17 alloy inertia friction welded joints

XU Hongji[1], YIN Lixiang[2], WEI Zhiyu[3], XIE Ming[1], ZHANG Tiancang[4] (1. School of Materials Science and Engineering, Dalian Jiaotong University, Dalian 116028, China; 2. Linde Engineering (Dalian) Co., Ltd, Dalian 116113, China; 3. Dalian CIMC Containers Co., Ltd, Dalian 116600 China; 4. Beijing Aeronautical Manufacturing Technology Research Institute, Beijing 100024, China). p 89—92

Abstract: The microstructures and properties of Ti17 alloy joints welded by inertia friction welding (IFW) were investigated by room-temperature tensile test, high-temperature tensile test and metallographic analyses. The results show that the joint with good performance at room and high temperature for Ti17 alloy can be obtained in IFW. Both the tensile strengths of welded joints at room temperature and at high temperature are not less than those of the base metal. The microstructure of Ti17 alloy is $\alpha+\beta$ phase, and the needle β phase is distributing on the α phase. While welding, different welding parameters can not affect the microstructures of the HAZ and the weld seam. The microstructure of HAZ is the same as that of the base metal, and that of the welded seam is fine equiaxed crystal.

Key words: Ti17 alloy; inertia friction welding; room-temperature tensile test; high-temperature tensile test